RNA (2002), *8*:1242–1252. Cambridge University Press. Printed in the USA.

DOI: 10.1017/S1355838202028066

A biosensor for theophylline based on fluorescence detection of ligand-induced hammerhead ribozyme cleavage

PHILLIP T. SEKELLA, DAVID RUEDA, and NILS G. WALTER
Department of Chemistry, University of Michigan, Ann Arbor, Michigan 48109-1055, USA

ABSTRACT

Recently, Breaker and coworkers engineered hammerhead ribozymes that rearrange from a catalytically inactive to an active conformation upon allosteric binding of a specific ligand. To monitor cleavage activity in real time, we have coupled a donor–acceptor fluorophore pair to the termini of the substrate RNA of such a hammerhead ribozyme, modified to cleave in *trans* in the presence of the bronchodilator theophylline. In the intact substrate, the fluorophores interact by fluorescence resonance energy transfer (FRET). The specific FRET signal breaks down as the effector ligand binds, the substrate is cleaved, and the products dissociate, with a rate constant dependent on the concentration of the ligand. Our biosensor cleaves substrate at 0.46 min^{-1} in 1 mM theophylline and 0.04 min^{-1} without effector, and discriminates against caffeine, a structural relative of theophylline. We have measured the theophylline-dependence profile of this biosensor, showing that concentrations as low as 1 μM can be distinguished from background. To probe the mechanism of allosteric regulation, a single nucleotide in the communication domain between the catalytic and ligand-binding domains was mutated to destabilize the inactive conformation of the ribozyme. As predicted, this mutant shows the same activity (0.3 min^{-1}) in the presence and absence of theophylline. Additionally, time-resolved FRET measurements on the biosensor ribozyme in complex with a noncleavable substrate analog reveal no significant changes in fluorophore distance distribution upon binding of effector.

Keywords: activity assay; asthma; bronchodilator; catalytic RNA; fluorescence resonance energy transfer; RNA conformational change

INTRODUCTION

Molecular recognition is an essential component in the regulation of all cellular processes, as it plays a critical role, for example, in the propagation of intra- and extracellular signals and in the activation and inhibition of metabolic enzyme activity. Therapeutically, it is important for the design and delivery of drugs as well as for their identification and quantification. To this end, the development of biosensors—tools that report the presence and concentration of a specific biomolecule—remains a challenging, yet important task for molecular engineers. Biosensors have extensive applications as the accurate detection and quantification of specific small molecules is essential throughout medicine and industry.

To date, much work has been invested into the development of antibody, protein enzyme, or receptor-based biosensors (for review, see, e.g., Scheller et al., 2001; Sapsford et al., 2002). Although these classes of biosensors are very successful at recognizing larger molecules such as other proteins, protein-based biosensors are less efficient at detecting small organic compounds. A particularly notorious target molecule is theophylline, a bronchodilator widely used in the treatment of asthma, bronchitis, and emphysema (Hendeles & Weinberger, 1983). Because of its narrow therapeutic index, serum levels must be monitored carefully to avoid toxicity. However, theophylline detection is particularly difficult because it is structurally very similar to the ubiquitous caffeine, which carries a single additional methyl group on N7 of the purine ring (Fig. 1B).

RNA provides a new avenue for the design of biosensors. RNA motifs termed “aptamers” that bind a small organic compound with high affinity and specificity can easily be obtained by in vitro selection (Wilson & Szostak, 1999). Due to the modularity of RNA struc-

Reprint requests to: Nils G. Walter, Department of Chemistry, University of Michigan, 930 N. University, Ann Arbor, Michigan 48109-1055, USA; e-mail: nwalter@umich.edu.

Abbreviations: FRET: fluorescence resonance energy transfer; trFRET: time-resolved fluorescence resonance energy transfer

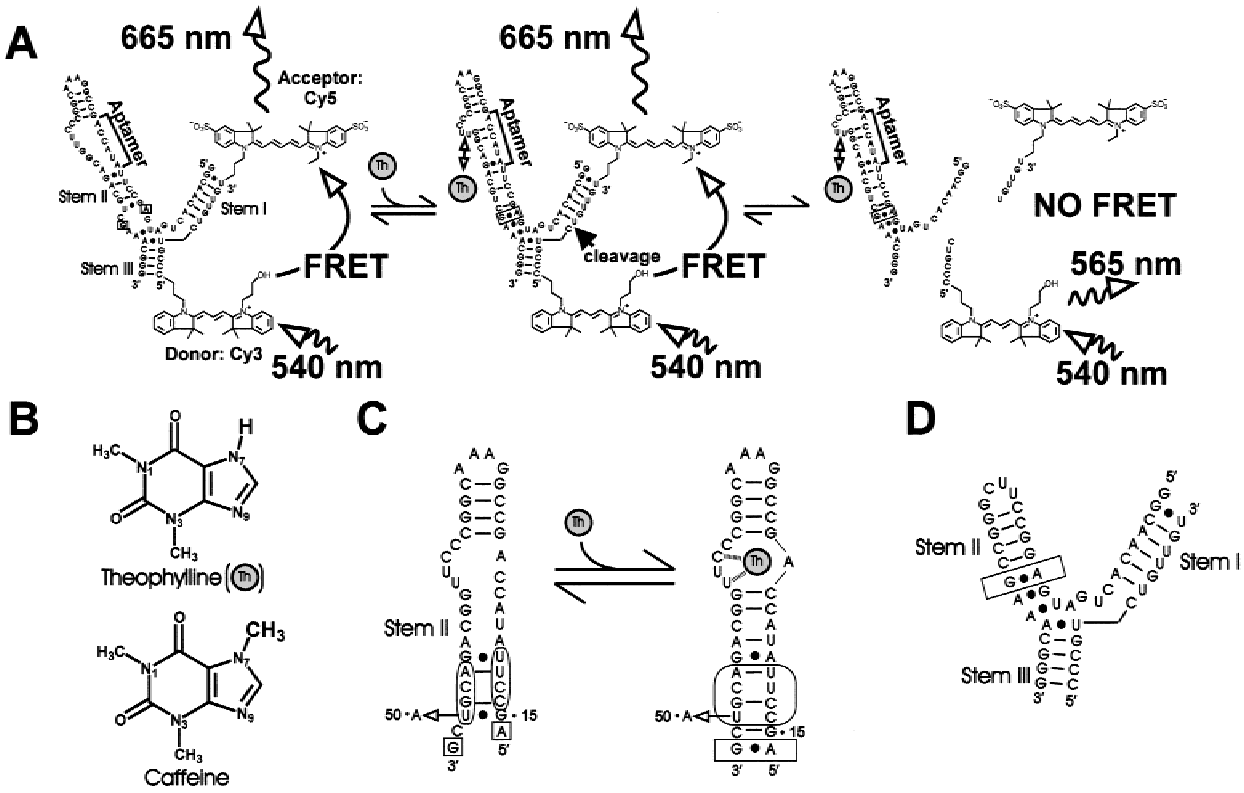

FIGURE 1. The hammerhead ribozyme as a biosensor for theophylline based on fluorescence resonance energy transfer (FRET). **A:** Ribozyme construct HHT1 and its activity. In the absence of theophylline, the ribozyme–substrate complex is in a catalytically inactive conformation characterized by a high FRET efficiency with strong acceptor emission at 665 nm (left). Upon addition of theophylline, the catalytically active conformation of the ribozyme, involving a noncanonical A:G base pair that is part of an essential metal-binding site (boxed; Wedekind & McKay, 1998), is stabilized. This local conformational change, however, does not result in any significant change in FRET (middle). Substrate cleavage is followed by the dissociation of the 5′ and 3′ products. The resulting separation of the fluorophores in solution decreases FRET so that the donor emission at 565 nm becomes dominant (right). **B:** Chemical structures of theophylline and caffeine, which differ only by a methyl group on N7 and can be distinguished by our biosensor. **C:** Details of the conformational change in stem II. In the absence of theophylline, the communication module (rounded boxes) is misaligned in a base-pairing pattern stabilized by the formation of a G_{15}:U_{50} wobble pair. With theophylline bound (specific hydrogen bonds are represented as hashed lines), the communication module is correctly aligned (rounded box), which allows formation of the catalytically active conformation. Mutation of U_{50} to A (yielding construct HHT2) destabilizes the inactive conformation of the ribozyme so that allosteric control is lost. **D:** Structure of stem II of control ribozyme HHR1 lacking the theophylline binding aptamer of HHT1. The boxed A:G pair is highlighted to show where HHR1 and HHT1 (**A** and **C**) begin to overlap in sequence.

tures, aptamers often retain their ligand-binding properties when incorporated into larger RNAs. With this principle in mind, Breaker and coworkers have engineered allosteric ribozymes that are comprised of three functional features: a specific aptamer motif, a hammerhead ribozyme catalytic core, and a structurally responsive communication domain between the two (Koizumi et al., 1999; Soukup & Breaker, 1999a, 1999b; Soukup et al., 2000, 2001). By incorporating the aptamer motif and the communication domain into Stem II of a hammerhead ribozyme (Fig. 1C), catalytic activity becomes responsive to binding of the aptamer ligand (Soukup & Breaker, 1999c, 2000). Such specific molecular switches can be used as biosensor components (Breaker, 2002).

A particular allosteric hammerhead ribozyme engineered by Breaker and coworkers is activated in the presence of theophylline, but not caffeine (Soukup & Breaker, 1999b). This ribozyme is 77 nt long and cleaves intramolecularly (in *cis*) with a rate constant of ~0.1 min^{-1} in 1 mM theophylline, which is ~100-fold faster than background cleavage in the absence of the cognate ligand. Breaker's group has recently utilized this and other allosteric hammerhead ribozymes as biosensor components (Breaker, 2002), by immobilizing an array of 5′-^{32}P-labeled ribozymes on a chip and analyzing them for loss of radioactivity by self-cleavage in the presence of a mixture of analytes. We set out to use the theophylline-activated ribozyme as a "parent" construct from which to develop a fluorescence-based biosensor.

Fluorescence methods are an attractive alternative to radioisotope detection for biosensor applications for a number of reasons, among them: (1) Fluorophore labeled RNA does not carry the risks inherent in the handling and disposal of radionuclides; (2) a fluores-

cence readout can directly monitor and quantify enzyme action in solution, making it inherently faster than the discontinuous analysis of a radioisotope assay; (3) fluorescence methods lend themselves to automation when used in conjunction with a microplate fluorescence reader; and (4) fluorescence probe shelf life is essentially unlimited.

Our biosensor for theophylline is designed to report ligand induced cleavage in *trans*, via fluorescence resonance energy transfer (FRET) between two related cyanine fluorophores. Cy3 (donor) and Cy5 (acceptor) are positioned on the 5′ and 3′ ends, respectively, of an external substrate (Fig. 1A). Dissociation of the reaction products generates a change in FRET signal and allows one to cost-effectively reuse the ribozyme by adding fresh substrate. The advantage of using spectroscopically active donor and acceptor fluorophores is that the ratiometric measurement of acceptor-to-donor fluorescence provides us with an automatic internal calibration.

FRET has been used extensively to study both cleavage kinetics and global conformational changes of catalytic RNA (Perkins et al., 1996; Bassi et al., 1997; Walter et al., 1998, 2002; Singh et al., 1999; Walter & Burke, 2000; Jenne et al., 2001; Walter, 2001; Pereira et al., 2002). We show here that FRET is also an excellent readout for biosensing. Our hammerhead ribozyme binds substrate rapidly and with high affinity at room temperature and shows enhanced, concentration-dependent cleavage activity in the presence of theophylline concentrations as low as 1 μM. This detection limit is highly suitable, as the nontoxic, therapeutic range of theophylline concentrations in blood plasma is between ~55 and 110 μM (10–20 μg/mL; Miyazawa et al., 2002). Furthermore, our biosensor is unaffected by millimolar concentrations of caffeine, and its reaction products dissociate rapidly, generating a real-time change in acceptor-to-donor fluorescence ratio upon substrate cleavage. FRET-based detection of ligand-induced cleavage by a hammerhead ribozyme therefore meets the essential criteria for specific and rapid detection and quantification of a medically relevant small organic compound.

RESULTS

Design of a fluorescence-based biosensor

To monitor its cleavage activity by FRET, several modifications were introduced to the theophylline-regulated parent hammerhead ribozyme (Soukup & Breaker, 1999b) to generate construct HHT1 (Fig. 1A). In particular, the originally *cis*-acting construct was disintegrated into ribozyme and external substrate strands to allow for efficient chemical synthesis of the fluorophore labeled substrate, and to create a rechargeable biosensor, capable of multiple turnover. In addition, the sequences of the substrate and the substrate-binding arms of the ribozyme were changed to those of a previously characterized hammerhead ribozyme (Michienzi et al., 2000). These sequence changes avoid self-complementarity of the original substrate strand, as predicted by Michael Zuker's RNA folding software "mfold version 3.0" (Mathews et al., 1999), and places an A:U base pair downstream of the cleavage site. This mutation is known to accelerate hammerhead ribozyme cleavage (Clouet-d'Orval & Uhlenbeck, 1997), so that the detection time for biosensing is decreased. As a theophylline-independent control construct, we designed a mutant ribozyme HHT2 that carries a U $\rightarrow$ A transversion in the communication domain (Fig. 1C). Finally, we designed a control ribozyme (termed HHR1) that has a shorter stem II lacking the aptamer motif (Fig. 1D).

RNA substrate binds rapidly and dissociates slowly

A reliable ribozyme-based biosensor should bind its substrate rapidly and with high affinity. To verify that our biosensor possesses such characteristics, we measured the rate constants of substrate binding and dissociation under standard single-turnover conditions (see Materials and Methods). Using a noncleavable, donor–acceptor doubly labeled substrate analog, we monitored substrate binding under varying ribozyme concentrations as a change in fluorescence signal. Addition of a 10-fold excess of ribozyme causes an increase in fluorescence of both the donor (Cy3) and acceptor (Cy5) fluorophores (Fig. 2A), presumably due to changes in their local quenching environments (Walter & Burke, 1997). In addition, the normalized ratio of Cy5-to-Cy3 emission, or relative FRET efficiency, decreases (Fig. 2A). This decrease indicates that the fluorophores are moving further apart; the substrate is going from a random coil in its unbound state to a pair of helices (stems I and III) in the ribozyme-substrate complex (Fig. 1A). The concentration of excess ribozyme was varied between 50 and 100 nM, and the time traces of relative FRET efficiency were each fit to a single-exponential decay function (see Materials and Methods). From the resultant concentration-dependent pseudo-first-order rate constants a bimolecular substrate binding rate constant k_{on} of $(1.09 \pm 0.02) \times 10^7$ min^{-1} M^{-1} was extracted for ribozyme HHT1 (Fig. 2B; Table 1). For the related ribozyme HHR1, which differs only by a shortened stem II (Fig. 1D), a ninefold faster bimolecular binding rate constant of $(9.9 \pm 0.6) \times 10^7$ min^{-1} M^{-1} was derived (Fig. 2B; Table 1). This faster binding rate may be due to the absence of the aptamer motif, which may slightly interfere with substrate binding to HHT1. Despite this apparent slowdown, HHT1 rapidly binds nanomolar substrate concentrations under our standard conditions, such that the ribozyme–substrate complex, or biosensor, is formed quickly (half-life ~25 s).

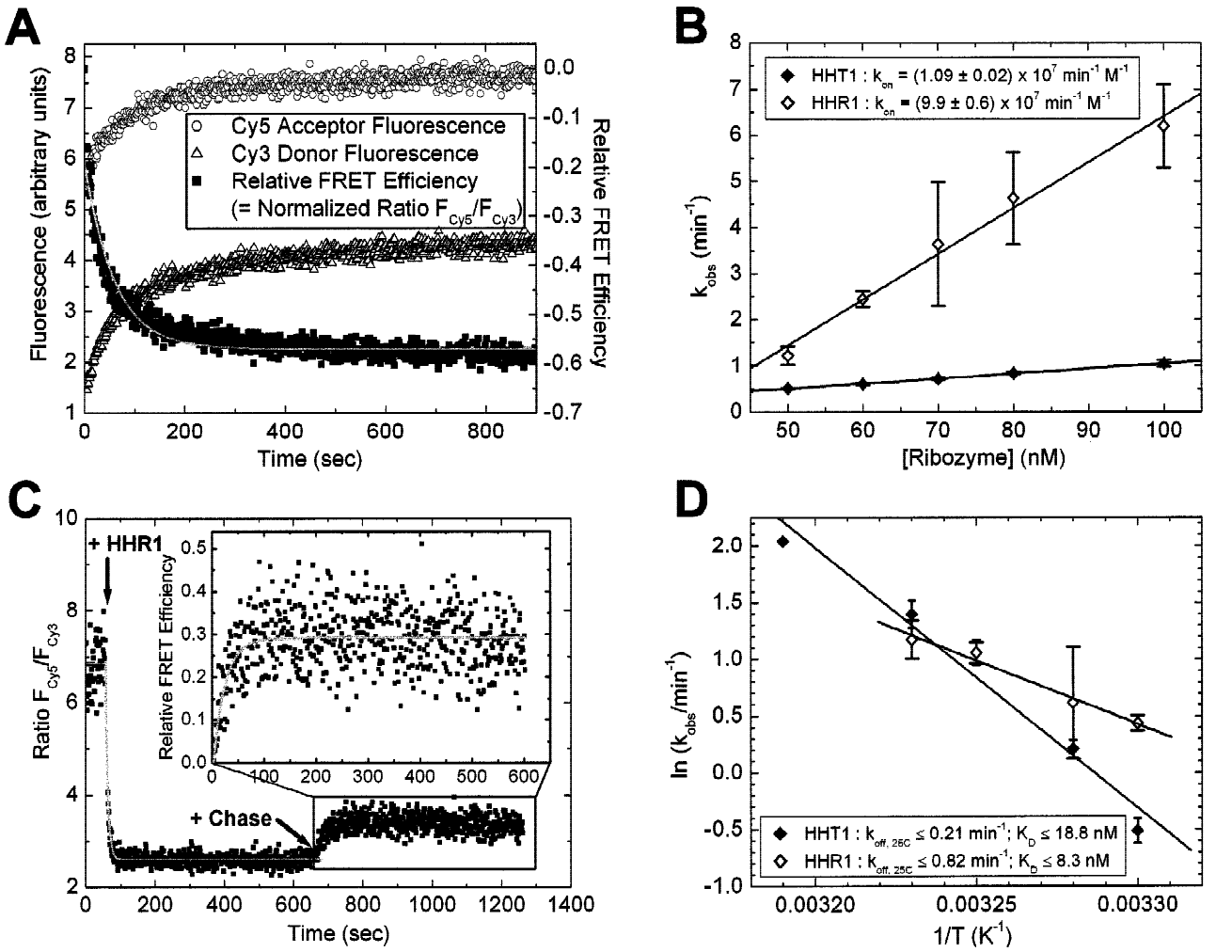

FIGURE 2. Measuring the rate constants of substrate binding and dissociation in standard buffer (50 mM Tris-HCl, pH 7.5, 10 mM $MgCl_2$, 25 mM DTT). **A:** Fluorescence and FRET time traces of 5 nM noncleavable substrate analog with terminal Cy3 and Cy5 labels upon addition of 100 nM HHT1 ribozyme at 25 °C. Although both the Cy5 and Cy3 fluorescence signals increase, the relative FRET efficiency decreases as the substrate binds to the ribozyme, forming stems I and III. The latter time trace yields a single-exponential decrease (gray line) with a pseudo-first-order rate constant k_{obs} of 1.01 min^{-1}, reported in **B**. **B:** Dependence on ribozyme concentration of k_{obs} from experiments such as the one in **A**. The slope of the linear regression lines yields the bimolecular substrate binding rate constants, k_{on}, of ribozymes HHT1 and HHR1, as indicated. **C:** Observing substrate dissociation at 35 °C. Upon addition of 100 nM ribozyme HHR1 to 5 nM noncleavable substrate analog, a decrease in acceptor-to-donor fluorescence ratio with a rate constant of 6.60 min^{-1} (gray line) indicates formation of the ribozyme–substrate complex. Then, 50 μM of a DNA substrate analog are added as chase to observe substrate dissociation; this results in a small increase in acceptor-to-donor fluorescence ratio by ~20% relative to the initial value of the unbound substrate. Inset: The time trace of relative FRET efficiency upon substrate dissociation yields a single-exponential increase (gray line) with a rate constant k_{obs} of 2.6 min^{-1}, reported in **D**. **D:** Arrhenius plot of the temperature dependence of the observed substrate dissociation rate constants derived from experiments such as the one in **C** over a range of 30 to 40 °C. Extrapolation yields an upper estimate for the dissociation rate constant k_{off} at 25 °C, as indicated. The ratio k_{off}/k_{on} then gives an upper estimate for the dissociation equilibrium constant K_D of the ribozyme–substrate complex.

To measure substrate dissociation, a large excess (10,000-fold, i.e., 50 μM) of an unlabeled DNA analog of the substrate was added as chase to the preformed ribozyme–noncleavable substrate analog complex. Yet at room temperature, no significant FRET change was observed (data not shown), implying that substrate does not dissociate significantly. To cause substrate dissociation in this chase assay, higher temperatures were applied and an Arrhenius plot (Fig. 2D) was used to extrapolate the dissociation rate constant at 25 °C. At these elevated temperatures, addition of 50 μM unlabeled DNA chase to the complex resulted in only a slight increase in relative FRET efficiency compared to the initial value of free substrate analog (see, e.g., the data at 35 °C, Fig. 2C). This observation indicates that only a fraction of ~20% of substrate dissociates from the ribozyme complex under these conditions. This fraction may represent a portion of the ribozyme–substrate

TABLE 1. Summary of kinetic parameters of the hammerhead ribozymes used in this study.[a]

	Ligand	HHT1	HHT2	HHR1
k_{cleav}^{fluor} (min^{-1})	1 mM theophylline	0.46 ± 0.01	0.30 ± 0.01	n.d.[b]
k_{cleav}^{fluor} (min^{-1})	None	0.04 ± 0.02	0.31 ± 0.02	n.d.
k_{cleav}^{fluor} (min^{-1})	1 mM caffeine	0.04 ± 0.02	n.d.	n.d.
K_M^{fluor} (μM)	Theophylline	200 ± 70	n.d.	n.d.
k_{cleav}^{radio} (min^{-1})	1 mM theophylline	0.47 ± 0.08	n.d.	n.d.
k_{cleav}^{radio} (min^{-1})	None	0.050 ± 0.002	n.d.	1.83 ± 0.02
k_{cleav}^{radio} (min^{-1})	1 mM caffeine	0.054 ± 0.001	n.d.	n.d.
K_M^{radio} (μM)	Theophylline	210 ± 70	n.d.	n.d.
k_{on}^{fluor} (10^7 min^{-1} M^{-1})	Substrate	1.09 ± 0.02	n.d.	9.9 ± 0.6
k_{off}^{fluor} (min^{-1})	Substrate	≤0.21	n.d.	≤0.82
K_D^{fluor} (nM)	Substrate	≤18.8	n.d.	≤8.3
k_{off}^{fluor} (min^{-1})	5′ product	4.3 ± 0.5	n.d.	5.2 ± 0.8

[a]All assays were performed as described in Materials and Methods under single-turnover conditions in standard buffer (50 mM Tris-HCl, pH 7.5, 10 mM $MgCl_2$, and 25 mM DTT, at 25 °C). Superscripts indicate whether the assay was fluorescence or radioactivity based.
[b]n.d. = not determined.

complex trapped in a less stable conformation, whereas 80% of the substrate appears inert with respect to substrate dissociation even at elevated temperature. Extrapolation to 25 °C thus yields an upper estimate for the substrate dissociation rate constant k_{off} of 0.21 min^{-1} for HHT1 and 0.82 min^{-1} for HHR1 (Fig. 2D; Table 1). The ratio of maximum substrate dissociation to the binding rate constant yields an upper estimate for the equilibrium dissociation constant, K_D, of 18.8 nM for HHT1 and 8.3 nM for HHR1 (Fig. 2D; Table 1). For a biosensor, a substrate K_D in the nanomolar to picomolar range is ideal for efficiency of detection so that the substrate binds rapidly but dissociates slowly; that is, bound substrate has a high probability to be cleaved rather than to dissociate, keeping the sensor in its "ready" state.

The products dissociate rapidly, so that substrate cleavage is rate limiting

To quantify the dissociation rate constant of the 5′ product (labeled with Cy3), a substantial excess of ribozyme (800 nM over 50 nM 5′ product) was required to saturate the change in Cy3 fluorescence upon formation of the ribozyme–5′ product complex. In the complex, Cy3 fluorescence increases (data not shown), similar to our observation for the substrate (Fig. 2A). To observe dissociation of 5′ product from this complex, a 1,000-fold excess (50 μM) of an unlabeled DNA analog of the 5′ product was added, resulting in a decrease in Cy3 fluorescence to its original level (Fig. 3). Quantification of the data yielded 5′ product dissociation rate constants k_{off} of 4.2 ± 0.5 min^{-1} for HHT1 and 5.2 ± 0.8 min^{-1} for HHR1 (Table 1). A similar experiment was attempted to quantify dissociation of the 3′ product. However, the ribozyme–3′ product complex proved to be very unstable and complex formation could not be observed. This instability implies that the binding affinity of the 3′ product is lower than that of the 5′ product, and that it dissociates faster. Because dissociation of the products after substrate cleavage is the event detected by fluorescence, such rapid dissociation of both products (at least 10-fold faster than cleavage) is ideal to ensure that theophylline-induced substrate cleavage, rather than product dissociation, is rate limiting for the overall reaction pathway (Fig. 1A).

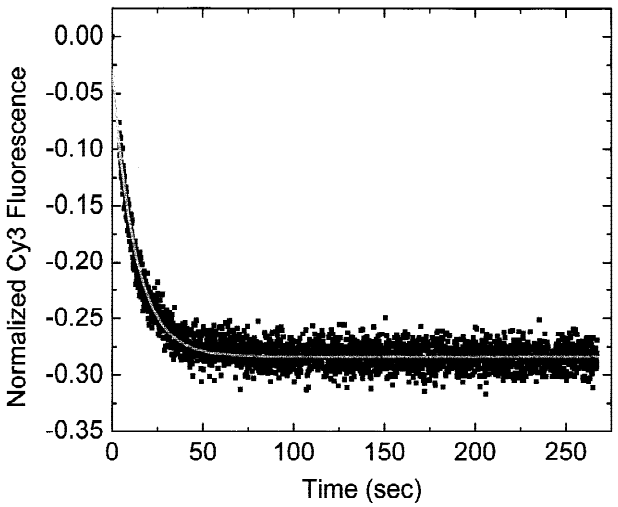

FIGURE 3. Fluorescence-based detection of dissociation of 5′ product from its complex with ribozyme HHT1 in standard buffer (50 mM Tris-HCl, pH 7.5, 10 mM $MgCl_2$, 25 mM DTT at 25 °C). Fifty-nanomolar Cy3-labeled 5′ product and 800 nM ribozyme were assembled into the ribozyme–5′ product complex. To observe dissociation of the ribozyme–5′ product complex, 50 μM of a DNA analog of the 5′ product were added as chase, resulting in a decrease in relative Cy3 fluorescence that can be fit with a single-exponential increase function (gray line) to yield a rate constant k_{off} of 4.8 min^{-1}.

The biosensor detects down to 1 μM theophylline

To evaluate the function of our allosterically controlled hammerhead ribozyme as a biosensor, single-turnover cleavage assays were performed to measure the sensitivity with which theophylline is detected in solution. For fluorescence assays, the ribozyme–substrate complex was formed as in the substrate binding assays. After the initial rapid signal decrease due to substrate binding, a slower FRET decrease at $\sim$0.04 min^{-1} (Table 1) was observed that is the result of residual ribozyme-mediated cleavage of substrate in the absence of specific aptamer ligand. After 10 min, analyte (i.e., theophylline) was added to the solution, and its presence was reported by the biosensor as an accelerated FRET decrease (Fig. 4). Under standard conditions (see Materials and Methods), theophylline concentrations as low as 1 μM were consistently distinguished from background as an increase in the rate constant of FRET change (Fig. 5A). Above 1 mM theophylline, this rate constant reached a plateau at 0.46 min^{-1}. Analyzing the rate constants of FRET change over this range of theophylline concentrations yielded an apparent equilibrium binding constant K_M for theophylline of 200 $\pm$ 70 μM. In contrast, the structurally similar caffeine (Fig. 1B) did not lead to a detectable rate enhancement above background (Fig. 4; Table 1).

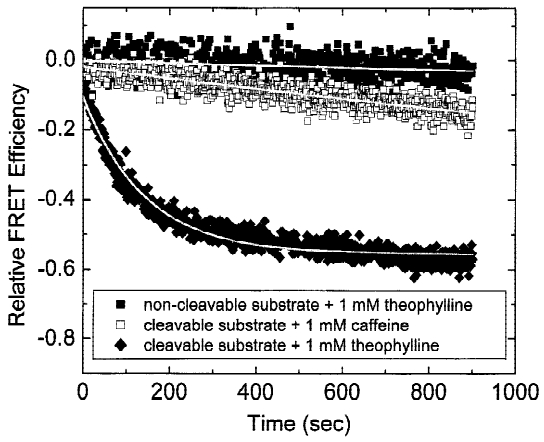

FIGURE 4. Change in relative FRET efficiency of the ribozyme–substrate complex of biosensor HHT1 upon addition of theophylline or caffeine in standard buffer (50 mM Tris-HCl, pH 7.5, 10 mM $MgCl_2$, 25 mM DTT at 25 °C). Addition of 1 mM theophylline to the ribozyme–noncleavable substrate analog complex does not significantly change the relative FRET efficiency (gray line, linear regression fit). Upon addition of 1 mM caffeine to the ribozyme–cleavable substrate complex, a slow decrease in relative FRET efficiency indicates residual background cleavage (the same decrease was observed when buffer was added instead). The data can be fit with a single-exponential decay function yielding a rate constant of 0.019 min^{-1} (gray line). Finally, addition of 1 mM theophylline to the ribozyme–cleavable substrate complex leads to a rapid decrease in relative FRET efficiency with a single-exponential rate constant of 0.42 min^{-1} (gray line).

To corroborate these data from FRET-based assays, standard radioactive cleavage assays were performed under similar reaction conditions. Cleavage occurred with a single-exponential rate to a final extent of 80–95%. The derived cleavage rate constants were very similar to those of the FRET assay between 1 μM and 1 mM theophylline, yielding a K_M for theophylline very similar to that of the FRET-based assays (210 $\pm$ 70 μM; Fig. 5B; Table 1).

Allosteric activation is mediated by a local change in base-pairing pattern

Breaker and coworkers proposed that a simple base-pairing change in the communication domain is responsible for the shift between the active and inactive conformations of the ribozyme (Soukup & Breaker, 1999b, 1999c; Fig. 1C). To verify this mechanism of allosteric activation, a new ribozyme, HHT2, was generated, with the 3′ most base in the communication domain, U_{50}, mutated to an A (Fig. 1C). This mutation was chosen to selectively destabilize the inactive, theophylline-free conformation of the ribozyme. In the original HHT1, U_{50} can make a G:U wobble pair with G_{15} to stabilize the inactive conformation of the ribozyme. By contrast, the mutant HHT2 can only form a less stable G:A pair in this position (Fig. 1C). Both FRET and radioactive cleavage assays show that HHT2 is constitutively active, with rate constants of 0.30 min^{-1} and 0.31 min^{-1} with and without theophylline, respectively (Table 1). Thus, a simple base-pairing change in stem II eliminates the allosteric regulatory properties of our biosensing ribozyme HHT1. This observation presents evidence that a localized base-pairing change in the communication domain of stem II, distal to the catalytic core, is responsible for partitioning the ribozyme between its active and inactive conformations (Fig. 1A).

To further corroborate this evidence, time-resolved FRET measurements were performed on the ribozyme–noncleavable substrate analog complex in the presence and absence of 1 mM theophylline to derive donor–acceptor fluorophore distances. Our analysis indicates that the distance distribution between Cy3 and Cy5 at the ends of stems I and III of the ribozyme–substrate complex (Fig. 1A) does not change significantly upon addition of theophylline (Fig. 6). This observation is also consistent with the idea that only a local change in base-pairing pattern activates catalytic activity, rather than a change in global structure. It should be noted that the observed mean fluorophore distances ($\sim$36 Å) are consistently smaller than expected from the hammerhead ribozyme crystal structures ($\sim$54 Å; Pley et al., 1994; Scott et al., 1995), which may indicate that the cyanine dyes are interacting with the RNA and become partially oriented (Norman et al., 2000; Klostermeier & Millar, 2001).

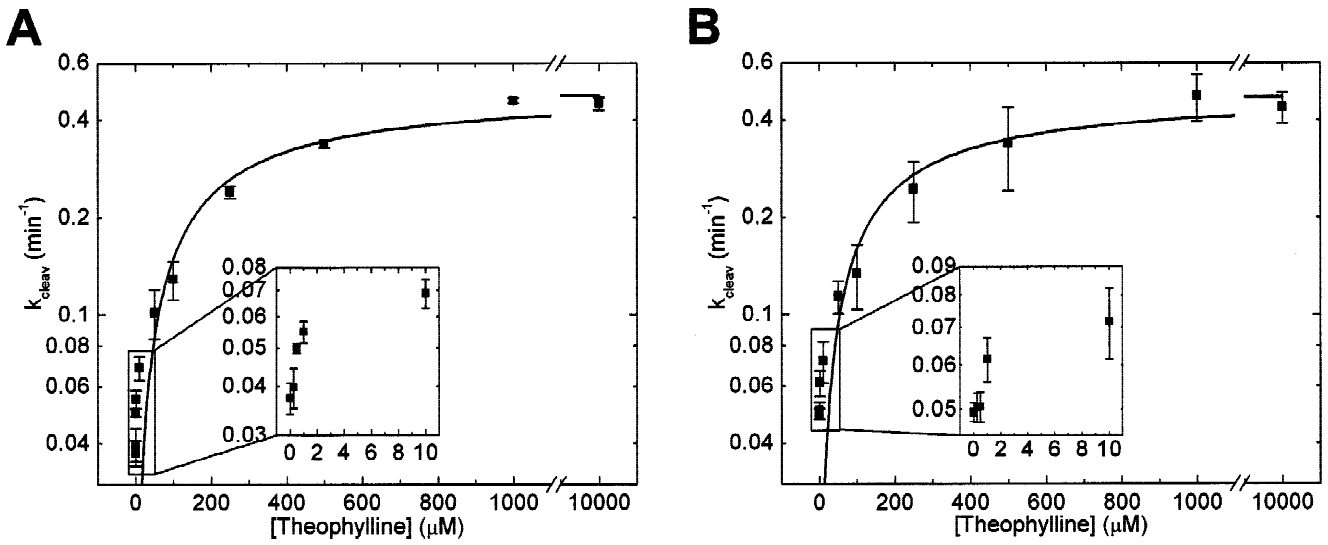

FIGURE 5. Increase in HHT1 biosensor activity with theophylline concentration. **A:** Rate constants obtained from steady-state FRET measurements. The line represents a fit with a binding equation (see Materials and Methods), yielding an apparent equilibrium binding constant K_M of 200 ± 70 μM. Inset: Theophylline concentrations as low as 1 μM can be distinguished from background cleavage in the absence of theophylline. Error bars arise from the standard deviation of three independent assays. **B:** Rate constants obtained from radioactive cleavage assays. The line represents a fit with a binding equation, yielding an apparent equilibrium binding constant K_M of 210 ± 70 μM. Inset: Theophylline concentrations as low as 1 μM are distinguishable from background. Error bars arise from the standard deviation of four independent assays.

DISCUSSION

The work presented here is based on the recent development of allosterically controlled hammerhead ribozymes as biosensor components (reviewed in Breaker, 2002). The relative ease of generating new aptamers by in vitro selection and the modularity of RNA structures make these self-cleaving ribozymes relatively straightforward to engineer (Koizumi et al., 1999; Soukup & Breaker, 1999a, 1999b, 1999c, 2000; Soukup et al., 2001, 2000). As an alternative to self-cleaving catalytic RNAs, self-ligating ribozymes have been proposed recently as biosensors that register the acquisition, rather than the loss, of a reporter RNA strand (Robertson & Ellington, 2000). To make use of either of these biosensors in high-throughput assays, a versatile, fast, and direct detection technique is needed for RNA cleavage and ligation. We have shown here that fluorescence resonance energy transfer (FRET) between a donor–acceptor fluorophore pair at the termini of an RNA substrate cleaved in *trans* provides for such a readout. FRET and fluorescence quenching effects enable us to readily measure substrate and product binding and dissociation rate constants to characterize the overall enzymatic reaction pathway of the biosensor. In addition, we have used mutational and time-resolved FRET analyses to provide evidence for a previously proposed structural mechanism of allosteric activation of the biosensing hammerhead ribozyme. Our studies present a proof of principle and can be directly transferred to other biosensors to be used in arrays (Seetharaman et al., 2001).

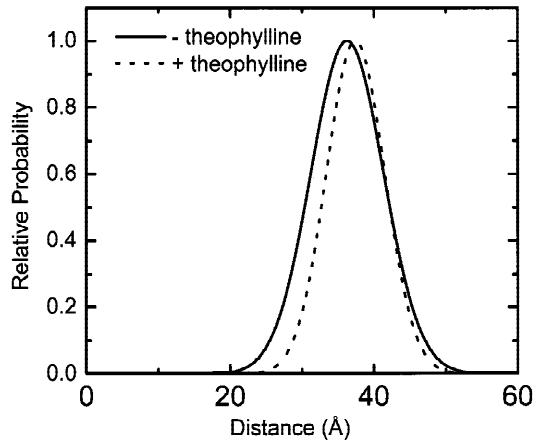

FIGURE 6. Time-resolved FRET analysis of structural changes of the HHT1-noncleavable substrate complex upon theophylline binding. In the absence of theophylline under standard conditions (50 mM Tris-HCl, pH 7.5, 10 mM $MgCl_2$, and 25 mM DTT at 25 °C), a Cy3-Cy5 fluorophore distance distribution with a mean distance of 36 ± 1 Å and a full width at half maximum (FWHM) of 12 ± 2 Å is observed (χ^2: 1.3). This distribution changes only slightly upon addition of 1 mM theophylline (mean distance: 37 ± 1 Å; FWHM: 9 ± 2 Å; χ^2: 1.3).

Recently, Jäschke and coworkers created a similar biosensor based on a theophylline-controlled hammerhead ribozyme cleaving an external substrate labeled with a fluorophore and a spectroscopically silent quencher (Frauendorf & Jaschke, 2001). This group reported only approximately fourfold allosteric activa-

tion by theophylline over background cleavage, but used units of temporal change in relative fluorescence that are not directly comparable to those used here or by Breaker and coworkers to characterize catalytic RNA function. The advantage of using a spectroscopically active acceptor fluorophore is that the ratiometric measurement of acceptor-to-donor fluorescence provides for an inherent calibration.

The modularity of RNA structure made it straightforward to create a *trans*-acting hammerhead ribozyme with a faster cleavage rate constant in the activated state than the original *cis*-acting ribozyme [0.46 min^{-1} (Table 1) versus 0.10 min^{-1} (Soukup & Breaker, 1999b)]. In particular, we incorporated an A:U base pair downstream of the cleavage site that was previously found to accelerate hammerhead ribozyme cleavage (Clouet-d'Orval & Uhlenbeck, 1997), possibly by facilitating a rate-limiting conformational change (Murray et al., 2002). Although the change in substrate sequence enhances activity in the presence of theophylline more than 4-fold, it also accelerates cleavage in the absence of the ligand 40-fold [0.04 min^{-1} (Table 1) versus 0.001 min^{-1} (Soukup & Breaker, 1999b)]; that is, although cleavage activity becomes faster and easier to detect by FRET, the dynamic range for catalytic function [i.e., the ratio of rate constants in the presence and absence of theophylline (Breaker, 2002)], drops ~9-fold. These observations are consistent with the notion that the allosterically controlled hammerhead ribozyme fluctuates between closely related conformational isomers, only some of which are catalytically productive, and that both theophylline binding in stem II as well as the presence of an A:U base pair downstream of the cleavage site increase the residence time of the ribozyme in the active state(s) (Fig. 1A). Consistent with this idea, the activity of control hammerhead ribozyme HHR1, which lacks the aptamer motif and thus is always in an active state (Fig. 1D), is faster still (1.83 min^{-1}; Table 1).

An ideal biosensor will have high catalytic activity in the presence of analyte to generate a fast reporter signal, and negligible activity in the absence of analyte to avoid false positives and keep the biosensor ready to report analyte binding (Breaker, 2002). With a cleavage rate constant of 0.46 min^{-1} in the presence of 1 mM theophylline, the half-life for substrate cleavage and thus signal generation by our current biosensor is ~90 s. A rate constant of 0.04 min^{-1} in the absence of theophylline determines the half-life of the biosensor in the "ready" state to ~1,000 s before substrate is lost to background cleavage. The dynamic range for detecting varying theophylline concentrations is determined by the gap in these half-lives. How can this gap be widened to improve dynamic range? Although the detection limit of our biosensor of ~1 μM theophylline and its apparent equilibrium binding constant of 200 μM (Table 1) make it highly suitable to detect the nontoxic, therapeutic range of theophylline concentrations in blood plasma [between ~55 and 110 μM (10–20 μg/mL; Miyazawa et al., 2002)], the ability of the isolated aptamer domain to bind theophylline with a K_D of 0.1 μM (Jenison et al., 1994) is not fully exploited. The reason probably lies in the fact that theophylline binding has to induce base-pair changes outside of the aptamer domain, particularly in the communication domain, to activate the catalytic domain of the hammerhead ribozyme (Fig. 1A). Recently, Breaker and coworkers optimized by in vitro selection the communication domain sequence of their theophylline-activated *cis*-cleaving hammerhead ribozyme with the goal of improving dynamic range (Soukup et al., 2000). A combination of such irrational design techniques with rational strategies will help to further improve performance of our fluorescence-based theophylline biosensor.

Homogeneous, real-time fluorescence assays like the one described here for theophylline detection have found widespread use in biotechnology for applications such as protein-based biosensors (van Roessel & Brand, 2002), real-time PCR quantification (Mackay et al., 2002), high-throughput screening (Hertzberg & Pope, 2000), and microarray analysis of gene expression (Blohm & Guiseppi-Elie, 2001; Schweitzer & Kingsmore, 2002), to name just a few. Microplate readers and high-density chip-based arrays are commonplace for fluorescence readout of many samples in parallel, and sophisticated real-time data analysis software has been developed. This existing technology can easily be transferred to our FRET-based RNA biosensor for further technological advancement. In addition, immobilizing the biosensor in a microplate will allow it to be recharged with fresh substrate after washing away cleavage products from a previous use. Finally, our choice of Cy3 and Cy5 as the donor–acceptor pair not only provides wide spectral separation of the donor and acceptor emission signals (565 nm versus 665 nm; Fig. 1A), but also lends itself to FRET measurements on single molecules (Zhuang et al., 2000, 2002), which present the smallest biosensors imaginable.

MATERIALS AND METHODS

Preparation of synthetic substrate RNA oligonucleotides and ribozyme HHR1

RNA oligonucleotides were purchased either from Dharmacon Research, Inc. or the HHMI Biopolymer/Keck Foundation Biotechnology Resource Laboratory at the Yale University School of Medicine (see Fig. 1 for sequences). Oligonucleotides were deprotected as suggested by the manufacturer. Deprotected RNA was purified by denaturing 20% polyacrylamide, 8 M urea gel electrophoresis. Bands of interest were diffusion eluted into 0.5 M NH_4OAc, 0.1% SDS, and 0.1 mM EDTA overnight at 4 °C, chloroform extracted, and ethanol precipitated. Pure RNA was isolated using C_8 reverse-phase HPLC with a linear acetonitrile gradient in triethylammonium

acetate as described previously (Walter, 2001). The RNA concentration was quantified by UV absorption at 260 nm with a correction for background at 320 nm. For fluorescence measurements, substrate oligonucleotides were labeled with Cy3 and Cy5 on the 5′ and 3′ ends pre- and postsynthetically, respectively, as previously described (Zhuang et al., 2002). For structural and kinetic studies, a noncleavable substrate analog was synthesized with the nucleotide 5′ to the cleavage site modified with a 2′-methoxy group to chemically block cleavage.

Transcription of HHT1 and HHT2

Upstream and downstream single-stranded DNA primers for transcription of both HHT1 and HHT2 constructs were purchased from Invitrogen with the following sequences: HHT1/HHT2 5′ primer: 5′-CAG *TAA TAC GAC TCA CTA TA*G GCA **ACA CTG ATG AGC CTT ATA CCA GCC GGA AAC G**-3′; HHT1 3′ primer: 5′-CCC GTT TCG ACG TCT GCC AAG GGC **CGT TTC CGG CTG GTA TAA GGC TCA TCA GTG T**-3′; HHT2 3′ primer: 5′-CCC GTT TCG TCG TCT GCC AAG GGC **CGT TTC CGG CTG GTA TAA GGC TCA TCA GTG T**-3′. The primer set for each construct contained a complementary internal sequence of 31 nt (boldfaced). Fully extended, double-stranded DNA for each construct template was generated by overlap-extension PCR in a reaction containing 2 μM of each primer, 0.3 mM each dNTP, 1.5 mM $MgCl_2$, 1× Reaction Buffer (10 mM Tris-HCl, pH 8.3, 50 mM KCl), and 0.05 U/μL recombinant Taq DNA polymerase (Takara). The reaction was incubated at 94 °C for 30 s, 55 °C for 30 s, 72 °C for 30 s, and cycled 5 times. PCR product was phenol/chloroform extracted and ethanol precipitated. Concentration of template DNA was quantified using UV absorbance as described above. Ribozymes HHT1 and HHT2 were then in vitro-transcribed from their respective PCR products using T7 RNA Polymerase. Two hundred nanomolar PCR product, containing the T7 promoter (sequence in italics), was incubated at 37 °C overnight in buffer containing ~6 U/μL T7 RNA polymerase purified from overexpressing *Escherichia coli* strain BL21/pAR1219 as previously described (Grodberg & Dunn, 1988), 5 U/mL inorganic pyrophosphatase (Sigma), 120 mM HEPES KOH, pH 7.6, 40 mM DTT, 30 mM $MgCl_2$, 2 mM spermidine, 0.01% Triton X-100, and 7.5 mM each rNTP. Reactions were concentrated to approximately 200 μL using Centricon Plus-20 centrifugal filters (Millipore). Two hundred microliters of gel loading buffer, containing 90% formamide, 0.025% xylene cyanol, and 0.025% bromophenol blue, were added and the samples were purified by denaturing 20% acrylamide, 8 M urea, gel electrophoresis. RNA was visualized using UV shadowing, and bands of interest were excised, diffusion eluted, chloroform extracted, ethanol precipitated, and their concentration determined as described above.

Steady-state FRET assays to observe hammerhead ribozyme cleavage

FRET-monitored cleavage assays were performed on an Aminco-Bowman 2 (AB2) spectrofluorometer (Thermo Spectronic). A final concentration of 50 nM Cy3-Cy5 donor–acceptor doubly labeled substrate was preincubated in a 150 μL cuvette at 25 °C in standard buffer: 50 mM Tris-HCl, pH 7.5, 10 mM $MgCl_2$, and 25 mM DTT as radical scavenger. Cy3 was excited at 540 nm (4 nm bandwidth) and fluorescence was monitored simultaneously at the Cy3 (565 nm, 8 nm bandpass) and Cy5 (665 nm, 8 nm bandpass) wavelengths by continuously shifting the emission monochromator between the two emission wavelengths. The ratio Q of Cy5 to Cy3 emission was calculated and normalized to its initial value Q_0 to yield a relative FRET efficiency ($(Q - Q_0)/Q_0$). Ribozyme HHT1 was folded by heating to 70 °C for 2 min in standard buffer and cooling to room temperature over 10 min. Ribozyme was added and manually mixed to give a final concentration of 200 nM (determined to be saturating by titration experiments). The binding of substrate to ribozyme was monitored for 10 min, allowing equilibrium to be reached. Theophylline was added and manually mixed to give final concentrations in the range of 250 nM to 10 mM. The theophylline-induced FRET change was monitored for 15 min. Rate constants were extracted by fitting to the single-exponential decay function $y = y_0 + Ae^{-x/t}$, using Microcal Origin 6.0 software; A is the amplitude and $1/t$ is the pseudo-first-order rate constant k_{obs}. Error bars arise from the standard deviation of three independent assays. An apparent equilibrium binding constant K_M for theophylline was derived by fitting plots of k_{obs} versus theophylline concentration with equation $y = k_{max}$ ([theo]/([theo] + K_M)), where k_{max} is the maximal rate constant.

Radioactive cleavage assays to observe hammerhead ribozyme cleavage

Radioactive cleavage assays were performed to confirm results of the FRET assays. 5′-^{32}P-labeled substrate was prepared from unmodified substrate RNA oligonucleotide by phosphorylation using T4 polynucleotide kinase (Promega) and [γ-^{32}P]ATP. Cleavage assays were conducted under single-turnover conditions with standard buffer identical to that used in FRET assays. 5′-^{32}P-labeled substrate and ribozyme were folded separately by heating to 70 °C for 2 min in standard buffer and allowing to cool to room temperature over 10 min. Reactions were initiated by mixing ribozyme and substrate. Aliquots of 5 μL were taken at particular time intervals and mixed with 10 μL of 90% formamide, 0.025% xylene cyanol, 0.025% bromophenol blue, 50 mM EDTA to quench the reaction. 5′ cleavage products were separated from uncleaved substrate by denaturing polyacrylamide, 8 M urea, gel electrophoresis and quantified using a Storm 840 PhosphorImager with ImageQuant software (Molecular Dynamics) as described previously (Pereira et al., 2002). Error bars arise from the standard deviation of four independent assays. Rate constants were extracted by fitting to a single-exponential decay function and an apparent equilibrium binding constant K_M was derived as described for the FRET assays.

Steady-state FRET assays to observe substrate binding and dissociation and product dissociation

Steady-state FRET assays were performed to measure the rate of substrate binding and dissociation as well as product dissociation for both HHT1 and HHR1. Ribozyme was folded

by incubation in standard reaction buffer at 70 °C for 2 min and allowed to cool to room temperature for 10 min. Cy3-Cy5 donor–acceptor doubly labeled, noncleavable substrate analog was incubated at 25 °C in standard reaction buffer, and Cy3 and Cy5 emission was monitored as described for the FRET-monitored cleavage assays. Ribozyme was added and manually mixed, and substrate binding was monitored as a decrease in relative FRET efficiency. For both HHT1 and HHR1, 5 nM noncleavable substrate analog was used, and ribozyme was added to give a final concentration ranging from 50 to 100 nM. Data were analyzed and rate constants extracted as described above. By plotting the pseudo-first-order rate constant k_{obs} as a function of ribozyme concentration, the bimolecular rate constant of substrate binding (k_{on}) could be determined from the slope of a linear fit using Microcal Origin 6.0.

Substrate dissociation is very slow and could not be quantified at room temperature. Instead, assays were performed at temperatures from 30 to 40 °C, where the ribozyme–substrate complex was less stable, and an Arrhenius plot was used to extrapolate the substrate dissociation rate at 25 °C (k_{off}). The ribozyme–noncleavable substrate complex was assembled as described above in standard reaction buffer. Five nanomolar substrate was incubated at a chosen temperature, and 100 nM ribozyme was added to form the bimolecular complex monitored as described above. Dissociation of the fluorescently labeled substrate was observed upon addition of 50 μM DNA oligonucleotide of the same sequence as the RNA substrate. Data were analyzed with Microcal Origin 6.0 as described above. An Arrhenius plot of the natural log of k_{obs} as a function of the inverse temperature yielded a linear fit that was used to extrapolate k_{obs} at 25 °C.

The ribozyme-5′ product complex was very unstable at 25 °C. Fifty nanomolar 5′ product labeled with Cy3 was mixed with 800 nM ribozyme, folded as described above. Product binding and dissociation were monitored by directly observing the fluorescence emission of Cy3 at 565 nm. Association resulted in an increase in Cy3 fluorescence, and dissociation resulted in a decrease in fluorescence. 50 μM of a DNA analog of the 5′ product were added to monitor dissociation of the Cy3-labeled 5′ product from the product–ribozyme complex. Data were analyzed as described above. Rate constants represent an average of three assays, and uncertainty arises from the standard deviation.

Time-resolved FRET measurements

The global structure of the doubly labeled HHT1 ribozyme–noncleavable substrate complex in the absence and presence of theophylline was studied by trFRET analysis similarly to previously described procedures (Walter et al., 1999; Pereira et al., 2002). Annealed ribozyme complex (70 μL; 1 μM doubly labeled noncleavable substrate analog, 3 μM ribozyme) was incubated at 25 °C for at least 15 min in standard buffer each in the absence and presence of 1 mM theophylline, followed by collection of the time-resolved donor emission profile using time-correlated single-photon counting. A frequency-doubled Nd:YVO_4 (Spectra-Physics Millenia Xs-P, operated at 9.0 W) pumped a frequency-doubled, mode-locked Ti:Sapphire laser (Spectra-Physics Tsunami, operated at 1 W) that excited Cy3 at 490 nm by 2-ps-width pulses, picked down to 4 MHz. Isotropic emission was detected at 568 nm (10-nm bandpass interference filter) in 4,096 sampling channels, with a time increment of 4.88 ps/channel, up to >40,000 peak counts and under magic angle polarizer conditions. To measure donor–acceptor distances, two time-resolved fluorescence decays were collected, with and without acceptor in place. The effect of the Cy5 acceptor on the decay of the Cy3 donor emission in the doubly labeled complex was then used to extract a three-dimensional Gaussian distance distribution between the two fluorophores as previously described in detail (Walter et al., 1999; Walter, 2001; Pereira et al., 2002). In all cases, a single distance distribution gave a good fit, as judged by the reduced χ^2 value ($\leq$1.3) and by evenly distributed residuals. To estimate a mean distance and full width at half maximum, a value of 47 Å for the Förster distance R_0 of Cy3 and Cy5 was used (Klostermeier & Millar, 2001), assuming random rotation of the two dyes. The latter assumption is probably an oversimplification (Norman et al., 2000; Klostermeier & Millar, 2001), leading to an underestimation of the actual fluorophore distance by ~30% (Pley et al., 1994; Scott et al., 1995).

ACKNOWLEDGMENTS

The authors wish to thank all members of the Walter group for stimulating discussions and David Millar, Steve Parus, and Steve Katnik for help with setting up our laser-induced time-resolved fluorometer. This work was supported by a grant from the National Institutes of Health (GM62357) to N.G.W. and a postdoctoral fellowship from the Swiss National Fonds to D.R.

Received May 21, 2002; returned for revision
June 19, 2002; revised manuscript received July 8, 2002

REFERENCES

Bassi GS, Murchie AI, Walter F, Clegg RM, Lilley DM. 1997. Ion-induced folding of the hammerhead ribozyme: A fluorescence resonance energy transfer study. *EMBO J 16*:7481–7489.

Blohm DH, Guiseppi-Elie A. 2001. New developments in microarray technology. *Curr Opin Biotechnol 12*:41–47.

Breaker RR. 2002. Engineered allosteric ribozymes as biosensor components. *Curr Opin Biotechnol 13*:31–39.

Clouet-d'Orval B, Uhlenbeck OC. 1997. Hammerhead ribozymes with a faster cleavage rate. *Biochemistry 36*:9087–9092.

Frauendorf C, Jaschke A. 2001. Detection of small organic analytes by fluorescing molecular switches. *Bioorg Med Chem 9*:2521–2524.

Grodberg J, Dunn JJ. 1988. ompT encodes the *Escherichia coli* outer membrane protease that cleaves T7 RNA polymerase during purification. *J Bacteriol 170*:1245–1253.

Hendeles L, Weinberger M. 1983. Theophylline. A "state of the art" review. *Pharmacotherapy 3*:2–44.

Hertzberg RP, Pope AJ. 2000. High-throughput screening: New technology for the 21st century. *Curr Opin Chem Biol 4*:445–451.

Jenison RD, Gill SC, Pardi A, Polisky B. 1994. High-resolution molecular discrimination by RNA. *Science 263*:1425–1429.

Jenne A, Hartig JS, Piganeau N, Tauer A, Samarsky DA, Green MR, Davies J, Famulok M. 2001. Rapid identification and characterization of hammerhead-ribozyme inhibitors using fluorescence-based technology. *Nat Biotechnol 19*:56–61.

Klostermeier D, Millar DP. 2001. Tertiary structure stability of the hairpin ribozyme in its natural and minimal forms: Different energetic contributions from a ribose zipper motif. *Biochemistry 40*:11211–11218.

Koizumi M, Soukup GA, Kerr JN, Breaker RR. 1999. Allosteric selection of ribozymes that respond to the second messengers cGMP and cAMP. *Nat Struct Biol 6*:1062–1071.
Mackay IM, Arden KE, Nitsche A. 2002. Real-time PCR in virology. *Nucleic Acids Res 30*:1292–1305.
Mathews DH, Sabina J, Zuker M, Turner DH. 1999. Expanded sequence dependence of thermodynamic parameters improves prediction of RNA secondary structure. *J Mol Biol 288*:911–940.
Michienzi A, Cagnon L, Bahner I, Rossi JJ. 2000. Ribozyme-mediated inhibition of HIV 1 suggests nucleolar trafficking of HIV-1 RNA. *Proc Natl Acad Sci USA 97*:8955–8960.
Miyazawa Y, Starkey LP, Forrest A, Schentag JJ, Kamimura H, Swarz H, Ito Y. 2002. Effects of the concomitant administration of tamsulosin (0.8 mg/day) on the pharmacokinetic and safety profile of theophylline (5 mg/kg): A placebo-controlled evaluation. *J Internat Med Res 30*:34–43.
Murray JB, Dunham CM, Scott WG. 2002. A pH-dependent conformational change, rather than the chemical step, appears to be rate-limiting in the hammerhead ribozyme cleavage reaction. *J Mol Biol 315*:121–130.
Norman DG, Grainger RJ, Uhrin D, Lilley DM. 2000. Location of cyanine-3 on double-stranded DNA: Importance for fluorescence resonance energy transfer studies. *Biochemistry 39*:6317–6324.
Pereira MJ, Harris DA, Rueda D, Walter NG. 2002. Reaction pathway of the *trans*-acting hepatitis delta virus ribozyme: A conformational change accompanies catalysis. *Biochemistry 41*:730–740.
Perkins TA, Wolf DE, Goodchild J. 1996. Fluorescence resonance energy transfer analysis of ribozyme kinetics reveals the mode of action of a facilitator oligonucleotide. *Biochemistry 35*:16370–16377.
Pley HW, Flaherty KM, McKay DB. 1994. Three-dimensional structure of a hammerhead ribozyme. *Nature 372*:68–74.
Robertson MP, Ellington AD. 2000. Design and optimization of effector-activated ribozyme ligases. *Nucleic Acids Res 28*:1751–1759.
Sapsford KE, Charles PT, Patterson CH Jr, Ligler FS. 2002. Demonstration of four immunoassay formats using the array biosensor. *Anal Chem 74*:1061–1068.
Scheller FW, Wollenberger U, Warsinke A, Lisdat F. 2001. Research and development in biosensors. *Curr Opin Biotechnol 12*:35–40.
Schweitzer B, Kingsmore SF. 2002. Measuring proteins on microarrays. *Curr Opin Biotechnol 13*:14–19.
Scott WG, Finch JT, Klug A. 1995. The crystal structure of an all-RNA hammerhead ribozyme: A proposed mechanism for RNA catalytic cleavage. *Cell 81*:991–1002.
Seetharaman S, Zivarts M, Sudarsan N, Breaker RR. 2001. Immobilized RNA switches for the analysis of complex chemical and biological mixtures. *Nat Biotechnol 19*:336–341.
Singh KK, Parwaresch R, Krupp G. 1999. Rapid kinetic characterization of hammerhead ribozymes by real-time monitoring of fluorescence resonance energy transfer (FRET). *RNA 5*:1348–1356.
Soukup GA, Breaker RR. 1999a. Design of allosteric hammerhead ribozymes activated by ligand-induced structure stabilization. *Structure Fold Des 7*:783–791.
Soukup GA, Breaker RR. 1999b. Engineering precision RNA molecular switches. *Proc Natl Acad Sci USA 96*:3584–3589.
Soukup GA, Breaker RR. 1999c. Nucleic acid molecular switches. *Trends Biotechnol 17*:469–476.
Soukup GA, Breaker RR. 2000. Allosteric nucleic acid catalysts. *Curr Opin Struct Biol 10*:318–325.
Soukup GA, DeRose EC, Koizumi M, Breaker RR. 2001. Generating new ligand-binding RNAs by affinity maturation and disintegration of allosteric ribozymes. *RNA 7*:524–536.
Soukup GA, Emilsson GA, Breaker RR. 2000. Altering molecular recognition of RNA aptamers by allosteric selection. *J Mol Biol 298*:623–632.
van Roessel P, Brand AH. 2002. Imaging into the future: Visualizing gene expression and protein interactions with fluorescent proteins. *Nat Cell Biol 4*:E15–E20.
Walter NG. 2001. Structural dynamics of catalytic RNA highlighted by fluorescence resonance energy transfer. *Methods 25*:19–30.
Walter NG, Burke JM. 1997. Real-time monitoring of hairpin ribozyme kinetics through base-specific quenching of fluorescein-labeled substrates. *RNA 3*:392–404.
Walter NG, Burke JM. 2000. Fluorescence assays to study structure, dynamics, and function of RNA and RNA-ligand complexes. *Methods Enzymol 317*:409–440.
Walter NG, Burke JM, Millar DP. 1999. Stability of hairpin ribozyme tertiary structure is governed by the interdomain junction. *Nat Struct Biol 6*:544–549.
Walter NG, Hampel KJ, Brown KM, Burke JM. 1998. Tertiary structure formation in the hairpin ribozyme monitored by fluorescence resonance energy transfer. *EMBO J 17*:2378–2391.
Walter NG, Harris DA, Pereira MJ, Rueda D. 2002. In the fluorescent spotlight: Global and local conformational changes of small catalytic RNAs. *Biopolymers 61*:224–242.
Wedekind JE, McKay DB. 1998. Crystallographic structures of the hammerhead ribozyme: Relationship to ribozyme folding and catalysis. *Annu Rev Biophys Biomol Struct 27*:475–502.
Wilson DS, Szostak JW. 1999. In vitro selection of functional nucleic acids. *Annu Rev Biochem 68*:611–647.
Zhuang X, Bartley LE, Babcock HP, Russell R, Ha T, Herschlag D, Chu S. 2000. A single-molecule study of RNA catalysis and folding. *Science 288*:2048–2051.
Zhuang X, Kim H, Pereira MJ, Babcock HP, Walter NG, Chu S. 2002. Correlating structural dynamics and function in single ribozyme molecules. *Science 296*:1473–1476.